Role of autophagy in a model of obesity: A long-term high fat diet induces cardiac dysfunction

YAN CHE[1-3*], ZHAO-PENG WANG[1-3*], YUAN YUAN[1-3], NING ZHANG[1-3],
YA-GE JIN[1-3], CHUN-XIA WAN[1-3] and QI-ZHU TANG[1-3]

[1]Department of Cardiology, Renmin Hospital of Wuhan University; [2]Cardiovascular Research Institute of Wuhan University;
[3]Hubei Key Laboratory of Cardiology, Wuhan, Hubei 430060, P.R. China

Abstract. Obesity may induce end-organ damage through metabolic syndrome, and autophagy serves a vital role in the pathogenesis of metabolic syndrome. The purpose of the present study was to define the roles of autophagy and mitophagy in high fat diet (HFD)-induced cardiomyopathy. Male, 8 week-old C57BL/6 mice were fed either a HFD (60% kcal) or a diet of normal chow (NC; 10% kcal) for 42 weeks. Glucose tolerance tests were performed during the feeding regimes. Blood samples were collected for assaying serum triglyceride with the glycerol-3-phosphate oxidase phenol and aminophenazone (PAP) method and total cholesterol was tested with the cholesterol oxidase-PAP method. Myocardial function was assessed using echocardiography and hemodynamic analyses. Western blot analysis was employed to evaluate endoplasmic reticulum stress (ERS), autophagy and mitochondrial function. Electron microscopy was used to assess the number of lipid droplets and the degree of autophagy within the myocardium. The body weight and adipose tissue weight of mice fed the HFD were increased compared with the NC mice. The serum levels of blood glucose, total cholesterol and triglyceride were significantly increased following 42 weeks of HFD feeding. The results of the glucose tolerance tests additionally demonstrated metabolic dysregulation in HFD mice. In addition, HFD mice exhibited hemodynamic and echocardiographic evidence of impaired diastolic and systolic function, including alterations in the cardiac output, end-diastolic pressure, end-diastolic volume and left ventricular relaxation time constant (tau) following HFD intake. Furthermore, a HFD resulted in increased ERS, and a downregulation of the autophagy and mitophagy level. The present study investigated cardiac function in obese HFD-fed mice. These results aid the pursuit of novel therapeutic targets to combat obesity-associated cardiomyopathy.

Introduction

Obesity, characterized by an excessive increase in body weight that results in excessive fat accumulation, is increasing at a high rate in all age groups (1,2). Obesity is associated with significant metabolic disturbances and leads to severe pathology in a number of organs, including the heart (3). Excessive fat intake limits metabolic flexibility for the mitochondrial production of adenosine 5'-triphosphate, which may lead to cellular injury and inflammation, and has been considered to be a major underlying factor in the pathogenesis of a number of diseases (4). In the heart, lipid overload has toxic effects and causes cardiac dysfunction (5). However, the mechanisms of lipotoxicity are not yet completely understood.

Autophagy is an evolutionarily conserved mechanism that maintains cellular and nutrient homeostasis by degrading misfolded proteins and damaged organelles, and has been identified as a major underlying factor in the pathogenesis of several chronic diseases (6,7). Dysregulation of autophagy may contribute to the development of cardiorenal metabolic syndrome including insulin resistance (8), hypertension and maladaptive immune modulation (9). A recent study focused on the role of autophagy in cardiovascular diseases and demonstrated that the role of autophagy is different in different cells and situations (10). Nevertheless, it remains unclear how a high-fat diet (HFD) influences the level of autophagy and the role it serves in obesity-associated cardiomyopathy. Furthermore, mitophagy as a special mode of autophagy is essential for the homeostasis of a healthy network of functioning mitochondria, and how it influences the hearts of HFD mice remains unclear. In the present study, a HFD was used to set up an obesity animal model to investigate the role of autophagy and mitophagy in the heart.

Materials and methods

Animal care and feeding. All the experimental procedures were approved by the Animal Care and Use Committee of

Correspondence to: Professor Qi-Zhu Tang, Department of Cardiology, Renmin Hospital of Wuhan University, 238 Jiefang Road, Wuhan, Hubei 430060, P.R. China
E-mail: qztang@whu.edu.cn

*Contributed equally

Renmin Hospital of Wuhan University (Wuhan, China), and were in accordance with the Guide for the Care of Laboratory Animals published by the US National Institutes of Health (publication no. 85-23, revised in 1996). The 8 week-old male C57BL/6 mice (n=30; weighing 22-24 g) purchased from the Institute of Laboratory Animal Science, Chinese Academy of Medical Sciences & Peking Union Medical College (Beijing, China) were randomly housed five mice/cage, given free access to water, and fed either a HFD (60% kcal fat; cat. no. D12492; Research Diets, Inc., New Brunswick, NJ, USA; n=15) or a normal fat diet (10% kcal fat; cat. no. D12450B; Research Diets, Inc.; n=15) for 42 weeks. Animals were housed in cages with a controlled temperature (22-25°C) and humidity (50±5%) and a 12/12 h light/dark cycle.

Hemodynamic analysis. During the hemodynamic measurement, a microtip catheter transducer (SPR-839; Millar, Inc., Houston, TX, USA) was inserted into the right carotid artery and advanced gradually into the left ventricle under anesthesia with 1.5% isoflurane. The signals were continuously recorded using a Millar Pressure-Volume system (MPVS-400; Millar, Inc.) and analyzed using PVAN data analysis software (version 3.5; Millar, Inc.). The cardiac output, end-diastolic pressure, end-diastolic volume and Tau_w (left ventricular relaxation time constant) were measured by pressure volume (PV) loop.

Measurement of random blood glucose and glucose tolerance test. Random blood glucose was measured once using a Relion Ultima diabetic glucometer (Abbott Diabetes Care, Abbott Park, IL, USA) using blood from the tail vein from normal chow (NC) (n=5) or HFD non-fasting mice (n=5).

Intraperitoneal glucose tolerance tests (IPGTT) were performed once at 50 weeks of age in all mice following 42 weeks of NC or HFD. Prior to the IPGTTs, mice were fasted for 6 h and then given a bolus of glucose (1.5 g glucose/kg body weight dissolved in sterile saline) by intraperitoneal injection. Blood samples were collected from the tail vein and assessed for glucose concentration prior to injection (0 min) and at 30, 60, 90, 120 and 150 min post-injection using a Relion Ultima diabetic glucometer (Abbott Diabetes Care; n=7 per group).

Blood collection. Mice were anesthetized with 1.5% isoflurane and the mouse orbital sinus was punctured with a capillary glass tube prior to the blood being collected (~400 μl/mouse) into a 1.5 ml Eppendorf tube. The samples were then centrifuged at 1,007 x g for 20 min at 4°C, and the serum was collected and stored at -80°C for use in further experiments.

Triglyceride (TG) and cholesterol (CHO) detection. The serum TG and CHO of non-fasting mice were measured using the TG (cat. no. A110-1) and CHO (cat. no. A111-1) assay kits, which was purchased from Nanjing Jiancheng Bioengineering Institute (Nanjing, China). All kits were used according to the manufacturer's protocol. The absorbance values at 510 nm were detected with a two-color infrared imaging system (Odyssey; LI-COR Biosciences).

Tissue protein extraction. Heart tissue extracts were collected from the mice by homogenizing the left ventricular samples in lysis buffer (50 mM Tris-HCl, 0.5% NP-40, 250 mM NaCl,

5 mM EDTA and 50 mM NaF). Subsequently, the protein concentration was measured with a bicinchoninic acid (BCA) protein assay kit using a microplate reader (Synergy HT; BioTek Instruments, Inc., Winooski, VT, USA). The proteins were subsequently collected and stored at -80°C for use in further experiments.

Mitochondria extraction. To determine the mitophagy level of mitochondria by western blotting, the isolation of mitochondria from cardiac tissues was performed using the Tissue Mitochondria Isolation kit (Beyotime Institute of Biotechnology, Beijing, China; cat. no. C3006). First, a fresh 50-mg left ventricular sample was washed once with PBS and placed in an ice bath in 500 μl pre-cooled PBS for 3 min, followed by centrifugation at 600 x g for 20 sec at 4°C, and the supernatant was discarded. Next, cardiac tissue was digested with 400 μl pre-cooled trypsin digestion solution for 20 min and centrifuged at 600 x g for 20 sec at 4°C. Subsequently, the tissue was resuspended with 100 μl mitochondrial separation reagent A and centrifuged at 11,000 x g for 10 min at 4°C, and the supernatant was discarded. Finally, 150 μl mitochondrial lysate was used to lyse the mitochondria and extract the mitochondrial protein. The protein concentration was measured using the BCA protein assay kit with a microplate reader (Synergy HT; BioTek Instruments, Inc.).

Western blot analysis. Heart tissue protein (80 μg) or cell protein (50 μg) were separately loaded onto 12, 10 or 8% SDS-PAGE gels and subsequently transferred onto Immobilon-FL transfer membranes (cat. no. IPFL00010; EMD Millipore, Billerica, MA, USA) in transfer buffer at 200 mA. The membranes were blocked with 5% non-fat milk at room temperature for 1 h and then incubated overnight at 4°C with specific antibodies. Anti-GAPDH (1:1,000; cat. no. 2118), C/EBP-homologous protein (CHOP; 1:500; cat. no. 2895), microtubule-associate proteins 1A/1B light chain 3-like protein (LC3-II/I; 1:500; cat. no. 12741), autophagy-related protein 7 (Atg7; 1:1,000; cat. no. 2613s) and phosphorylated (p)-sequesteosome-1/(P62; 1:500; cat. no. 13121s) were purchased from Cell Signaling Technology, Inc., (Danvers, MA, USA). Beclin-1 (1:500; cat. no. ab55878), parkin (1:1,000; cat. no. ab15954), mitofusin2 (1:1,000; cat. no. ab56889), serine/threonine-protein kinase PINK1 mitochondrial (PINK1; 1:1,000; cat. no. ab186303) and voltage-dependent anion-selective channel protein 1 (VDAC1; 1:1,000; cat. no. ab191440) were purchased from Abcam (Cambridge, UK). Peroxisome proliferator-activated receptor-α (PPARα; 1:1,000; cat. no. sc-9000), x-box-binding protein-1 (XBP-1; 1:500; cat. no. sc-7160) and glucose-regulated protein 78 (GRP78; 1:500; cat. no. sc-13968) were purchased from Santa Cruz Biotechnology, Inc., (Dallas, TX, USA). Subsequently, the membranes were incubated with IRDye 800CW conjugated goat anti-mouse IgG (cat. no. P/N 925-32210; 1:1,250; LI-COR Biosciences, Lincoln, NE, USA) and goat anti-rabbit IgG (cat. no. P/N 925-32211; 1:1,250; LI-COR Biosciences) for 1 h at room temperature. The blots were subsequently probed using Odyssey Software (version 3.0; LI-COR Biosciences).

Scanning electron microscopy (SEM). Freshly isolated heart tissues were fixed with 2.5% glutaraldehyde in phosphate

buffer (pH 7.0) at 4°C for 8 h and then delivered to the electron microscopy facility of the Renmin Hospital of Wuhan University for post-processing. Briefly, following three washes in phosphate buffer (pH 7.4) for 10 min at 4°C, tissues were fixed for 90 min in a 1.0% OsO_4 solution at 4°C, prepared with the phosphate buffer (pH 7.4). Tissues were then rehydrated in a descending alcohol series and sputter coated with silver ions. Finally, SEM observations were performed using a scanning electron microscope (TM-3000; Hitatchi, Ltd., Tokyo, Japan). Micrographs were captured in a blinded manner at magnifications of x3,000, x5,000 and x8,000.

Cell culture and treatment. H9C2 cells, purchased from the Cell Bank of Type Culture Collection of Chinese Academy of Sciences (Shanghai, China), were cultured in Dulbecco's modified Eagle's medium (Gibco; Thermo Fisher Scientific, Inc., Waltham, MA, USA) with 10% fetal bovine serum (Chinese Academy of Sciences, Shanghai, China) at a temperature of 37°C and 5% CO_2. The cells ($1x10^6$ cells/well) were transfected in 6-well plates and allowed to adhere for 24 h. Cells were left untreated or were treated with 400 μM palmitate (PA; Sigma-Aldrich; Merck KGaA, Darmstadt, Germany) for 24 h at a temperature of 37°C. To regulate autophagy, the autophagy inhibitor bafilomycin A1 (Baf A1; 50 nM; Sigma-Aldrich; Merck KGaA) was added for 1 h prior to the addition of 400 μM PA and incubation for 24 h. Cellular proteins were extracted for the detection of autophagy using western blot according to the aforementioned protocol. Lysis buffer (50 μl) was added to each well, and proteins were extracted according to the aforementioned protocol.

Monomeric cherry (mCherry)-green fluorescent protein (GFP)-LC3 adenovirus transfection and confocal microscopy. A plasmid-encoded tandem mCherry-GFP-LC3 construct adenovirus was purchased for the quantification of autophagic maturation from ViGene Biosciences (Rockville, MD, USA). Cells ($5x10^5$/ml; 500 μl/well) were seeded onto a 24-well plate with chamber slides placed below and allowed to adhere for 24 h. Following the addition of $5.0x10^{-3}$ mg/ml ADV-HR to improve the efficiency of transfection, H9C2 cells were simultaneously transfected with mCherry-GFP-LC3 adenovirus (both ViGene Biosciences Inc., Rockville, MD, USA; $1.0x10^{10}$ plaque forming units/ml; 0.5 μl/well) according to the manufacturer's protocol and cultured at 37°C and 5% CO_2 for 2 h. The medium was replaced with fresh complete culture medium and the cells were incubated for another 24 h prior to the addition of Baf A1. Following 1 h, the cells were untreated or treated with 400 μM PA for 24 h. Following removal of the culture media and washing with 1% Triton X-100 in PBS with 0.1% Tween-20 for 15 min at room temperature, the cells were stained with 300 nM 4',6-diamidino-2-phenylindole dihydrochloride (Invitrogen; Thermo Fisher Scientific, Inc.) for 5 min at room temperature. Images were obtained using an Olympus confocal microscope (Olympus Corporation, Tokyo, Japan), with a magnification of x400. A minimum of 10 fields of view were observed per sample.

Statistical analysis. All results are presented as the mean ± standard error of mean. Unpaired two-tailed Student's t-test was used to determine differences between the means of the HFD and NC groups. One-way analysis of variance (ANOVA) was used to analyze multiple groups and Bonferroni's post-hoc testing was employed following ANOVA for testing significant differences between groups. Glucose tolerance was assessed by calculating the area under the curve. All statistical analyses were performed using SPSS 17.0 software (SPSS, Inc., Chicago, IL, USA). Figures were compiled using GraphPad Prism 6.02 software (GraphPad software, Inc., La Jolla, CA, USA). All experiments were repeated in triplicates. P<0.05 was considered to indicate a statistically significant difference.

Results

HFD causes pathological obesity in mice. Male mice were fed either NC or a HFD for 42 weeks starting at 8 weeks of age. The long-term consumption of a HFD caused a significantly increased body and heart weight compared with the NC group (P<0.05; Fig. 1A and B). Additionally, HFD-fed mice exhibited a significant increase in body fat and lean body mass percentage compared with the NC diet (P<0.05; Fig. 1C). The levels of TG, CHO and glucose were significantly increased, which indicated there was a metabolic disturbance in the HFD mice (P<0.05; Fig. 1D-F). Furthermore, the HFD-exposed mice exhibited an impaired glucose tolerance level (Fig. 1E and F).

HFD causes cardiac dysfunction in mice. The cardiac function of NC and HFD mice was evaluated by PV loop (Fig. 2A) following 42 weeks of feeding. The results of the PV loop analysis revealed that HFD damaged systolic and diastolic cardiac functions. In the HFD mice, cardiac output was significantly decreased (P<0.05; Fig. 2B), indicating systolic dysfunction. In addition, the end-diastolic pressure significantly increased (P<0.05; Fig. 2C) although end-diastolic volume decreased (Fig. 2D) in the HFD mice compared with the NC mice, indicating significant cardiac diastolic dysfunction. Tau_w, a further indicator of diastolic function of the heart, was significantly increased in HFD mice (P<0.05; Fig. 2E). These results suggested that HFD induced cardiac dysfunction of systole and diastole.

ERS is upregulated during obesity. PPARα is associated with dyslipidemia and cardiovascular disease (11). The level of PPARα was tested, and the results demonstrated that the level of PPARα significantly increased following HFD feeding compared with the NC group (P<0.05; Fig. 3). As the reduction of PPARα expression may inhibit ERS (12), the level of ERS was tested. During ER stress, the level of CHOP expression is elevated and its role in programmed cell death of ER-stressed cells is correlated with its role in promoting protein synthesis and oxidative stress inside the ER (13). GRP78, additionally termed binding immunoglobulin protein, is a heat shock protein 70 molecular chaperone located in the lumen of the ER that binds newly synthesized proteins as they are translocated into the ER. When protein folding is disturbed inside the ER, GRP78 synthesis is increased (14). XBP-1 is a well-conserved component of the unfolded protein response, which is crucial for glucose homeostasis and lipid metabolism (15). A HFD increased the protein expression of CHOP, XBP-1 and GRP78 (Fig. 3), indicating activation of ERS.
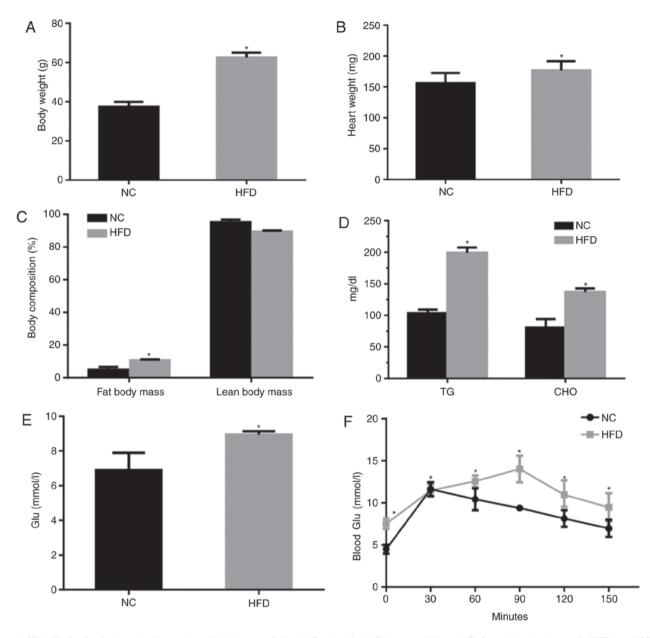
Figure 1. High-fat feeding leads to obesity and metabolic abnormalities. (A) Body weight, (B) heart weight, and (C) fat and lean body mass in HFD- and NC-fed mice. Fat mass=visceral fat + epididymal fat; lean mass=body weight-fat mass. (D) CHO and TG levels in mice measured following 42 weeks of NC or HFD feeding. (E) Random blood Glu, n=5 mice per group. (F) Glu tolerance test, n=7 mice per group. Values are expressed as the mean ± standard error of the mean. *P<0.05 vs. NC. CHO, cholesterol; TG, triglycerides; NC, normal chow; HFD, high fat diet; Glu, glucose.

HFD-induced obesity impairs autophagy. According to a previous study using hepatocytes, ERS may trigger ER-associated degradation and autophagy, which can clear unfolded proteins and restore protein homeostasis (16). Therefore the influence of a HFD on autophagy was tested. To study the role of autophagy in HFD-induced cardiac dysfunction, the expression of autophagy-associated proteins in the heart was analyzed. During autophagy, LC3-I is converted to LC3-II through lipidation by the ubiquitin-like system involving Atg7. This process allows for LC3 to become associated with autophagic vesicles, whose membranes are marked by P62 (17), and levels of LC3-I and P62 may be decreased when autophagic flux is unobstructed. Beclin-1 is critical to autophagy as it may stimulate autophagy when overexpressed in mammalian cells (18). In the present study, HFD induced a significant upregulation of Atg7, beclin-1 and

P62, although it downregulated the level of LC3-II/I compared with the NC group. These imbalances in protein expression involved in autophagy confirmed that autophagy was impaired in the HFD-fed mice (Fig. 4A and B). Consistent with the results of the western blotting, electron microscopy demonstrated an increased number of lipid droplets and autophagosomes in HFD-fed mice compared with the NC group (Fig. 4C and D), which indicated that there was no barrier to the formation of autophagosomes. However, there were fewer autolysosomes in HFD-fed mice, which indicated that there was inhibition of autophagosome degradation. These results may explain the cause of the increase in P62.

Impairment of autophagic flux in H9C2 cells treated with PA. To investigate the autophagic process involved in HFD, the protein expression of LC3 and P62 was tested by
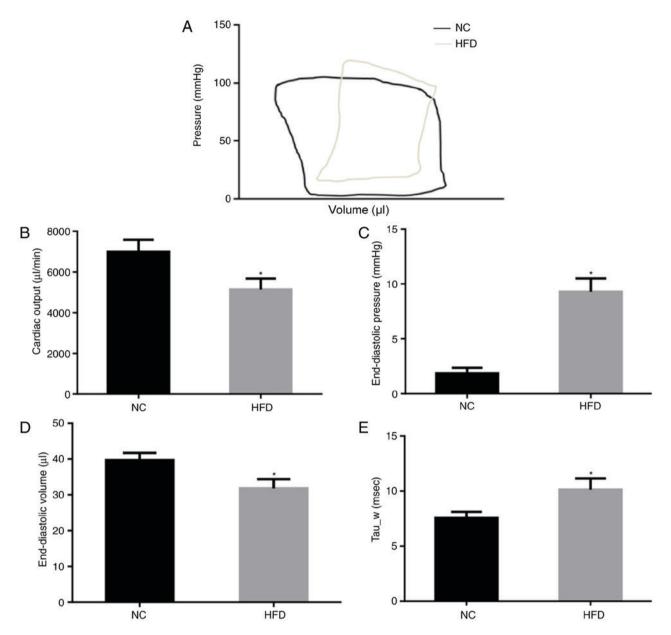
Figure 2. Cardiac function data and hemodynamic parameters following 42 weeks of HFD feeding. (A) Pressure volume-loop: The systolic and diastolic functional indexes of (B) cardiac output. (C) End-diastolic pressure. (D) End-diastolic volume. (E) Tau_w. Data are presented as the mean ± the standard error of the mean, n=5-6 samples per group. *P<0.05 vs. NC. NC, normal chow; HFD, high fat diet; Tau, left ventricular relaxation time constant.

western blotting *in vitro*. The results of the western blotting demonstrated that PA, a primary product of fatty acid synthase, may increase LC3-II/I in the presence of Baf A1 (Fig. 5A), an autophagic inhibitor which prevents the maturation of autophagic vesicles by inhibiting the fusion between lysosomes and autolysosomes. Furthermore, P62 expression was altered when treated with PA, Baf A1 and the two together (Fig. 5B).

To clarify whether autophagic flux was influenced by PA, mCherry-GFP-LC3, a tandem fluorescent indicator was used. Since the green fluorescence of the fusion protein is sensitive to the acidic environment of lysosomes and is quickly quenched in autolysosomes, only red fluorescence was detectable in the autolysosomes. Therefore, when lysosomal degradation was inhibited by treating the cells with Baf A1, an accumulation of green puncta was observed (Fig. 6A and B), which is consistent with PA-induced cells. Notably, an increase in green puncta

was observed in Baf A1+PA treated cells compared with the other groups. These results suggested that PA inhibited autophagic flux via suppression of lysosomal degradation.

HFD-induced obesity impairs the regulation of mitochondrial quality control. Mitochondria are essential organelles that serve important roles in cellular energy metabolism. The mitochondrial quality control systems that have evolved to repair or eliminate dysfunctional mitochondria are of importance (19). Furthermore, mitochondrial quality surveillance systems attenuate potentially damaging processes that occur in the cytosol and ER (20). As a part of mitochondrial quality surveillance systems, mitophagy may selectively engulf and clear mitochondria, thus mitophagy is essential for the homeostasis of a healthy network of functioning mitochondria. In the course of mitophagy, PINK1 and the E3 ubiquitin ligase parkin act as synergistic mediators (21). In response to mitochondrial
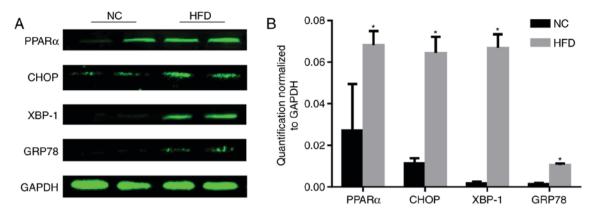
Figure 3. HFD induces endoplasmic reticulum stress. (A) The protein expression of PPARα, CHOP, XBP-1, GRP78 and GAPDH in the cardiac tissues determined by western blot analysis. (B) Quantification normalized to GAPDH demonstrated that HFD induced the level of endoplasmic reticulum stress. n=4 per group. *P<0.05 vs. respective NC. NC, normal chow; HFD, high fat diet; PPARα, peroxisome proliferator-activated receptor α; CHOP, C/EBP-homologous protein; XBP-1, X-box binding protein-1; GRP78, glucose regulated protein 78.
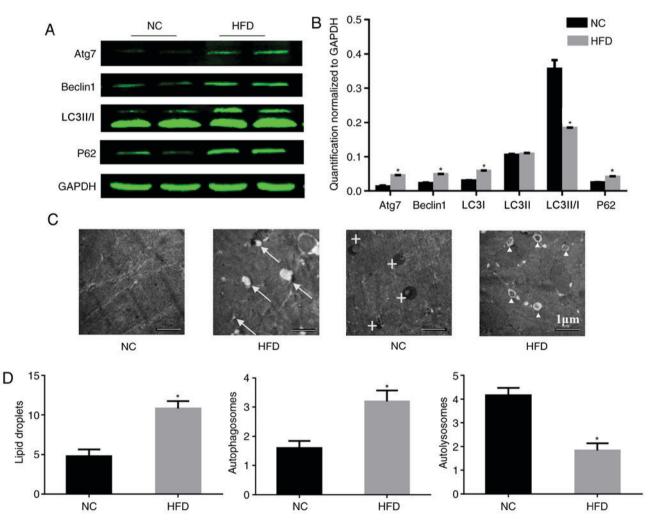

Figure 4. HFD reduces the level of autophagy in heart tissue. (A) Protein expression of Atg7, beclin-1, LC3-II/I, P62 and GAPDH, and (B) quantification. n=4 per group. (C) Representative electron micrographs of the cardiac muscle from the septum identified lipid droplets in only the HFD mice, and there were more autophagosomes existing in the HFD mice. Original magnification, x5,000. The arrows mark lipid droplets around cardiomyocytes, crosses mark autolysosomes and triangles mark autophagosomes. (D) Quantitative analysis of lipid droplets, autophagosomes and autolysosomes in the images. n=2 per group. *P<0.05 vs. respective NC. NC, normal chow; HFD, high fat diet; Atg7, autophagy-related protein 7; LC3-II/-I, MAP1 light chain 3-like protein III/I; P62, sequesteosome-1.

depolarization, PINK1 accumulates on the mitochondrial outer membrane, which subsequently recruits parkin from the cytosol and activates its ubiquitin ligase activity to eliminate damaged mitochondria (22). Furthermore, mitochondrial
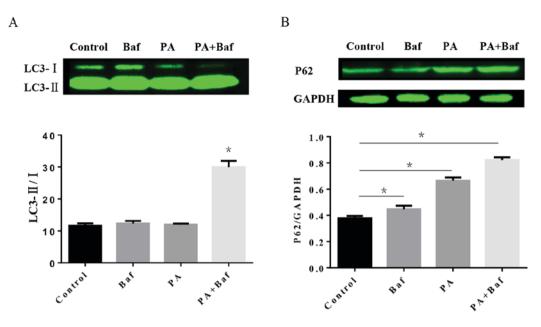
Figure 5. PA impaired the formation of autolysosome. (A) Protein expression of LC3-II/I in cells treated with or without PA (400 μM) and Baf (50 nM) in H9C2 cells and quantitative, n=3 per group. (B) Protein expression of P62 in cells and quantitative, n=3 per group. *P<0.05. PA, palmitate; Baf, bafilomycin A1; LC3-II/I, MAP1 light chain 3-like protein II/I.
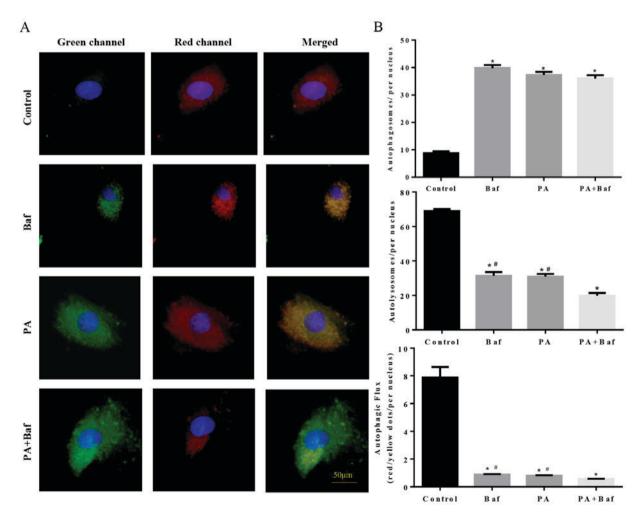

Figure 6. Transfection of the mCherry-GFP-LC3 plasmid into H9C2 cells and quantification of the autophagic puncta by confocal microscopy. (A) H9C2 cells were cultured under normal conditions (Control), in the presence of Baf A1 (Baf), palmitate (PA) and the two combined (Baf+PA). Representative epifluorescence images (x400) demonstrated the cellular localization of mCherry-GFP-LC3 in the H9C2 cells. (B) The mean number of autophagosomes and autolysosomes are represented by yellow and red dots, respectively, in the merged images. The results represent the means from at least three independent experiments and at least six cells in each group were counted. The results are presented as the mean ± the standard error of the mean. *P<0.05 vs. control and #P<0.05 vs. PA+Baf by post-hoc test. PA, palmitate; Baf, bafilomycin A1; GFP, green fluorescent protein.
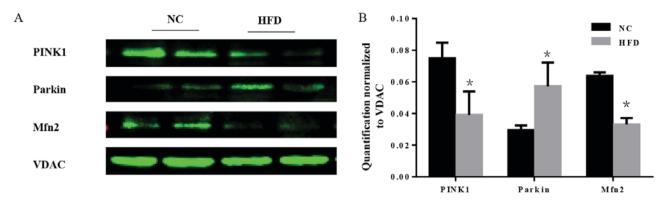
Figure 7. HFD-induced obesity impairs the regulation of mitochondrial quality control. (A) Protein expression of PINK1, parkin, Mfn2 and VDAC in heart tissues. (B) Quantification normalized to VDAC demonstrates the decrease in mitophagy and fusion in obese mice. n=4 per group. *P<0.05 vs. respective NC. NC, normal chow; HFD, high fat diet; PINK1, serine/threonine-protein kinase PINK1 mitochondrial; Mfn2, mitofusin2; VDAC, voltage-dependent anion channel 1.

fusion is a part of mitochondrial quality surveillance systems, and mitofusin 2 (Mfn2) is a mitochondrial membrane protein that is involved in mitochondrial fusion in mammalian cells (23). The expression level of PINK1, parkin and Mfn2 was tested. The results demonstrated that there was a significant increase in parkin, and a significant decrease in PINK1 and Mfn2 in HFD mice compared with the NC group (P<0.05; Fig. 7), which indicated that the mitochondrial quality surveillance system was dysfunctional.

Discussion

In the present study mice were fed with a HFD for 42 weeks to investigate the influence of obesity on the heart. During the *in vivo* study, a HFD was observed to induce obesity and lead to metabolic abnormalities and cardiac function deterioration. In addition, it was also demonstrated that ERS was increased in long-term HFD mice. Furthermore, autophagy and mitophagy in the obese mouse heart were dysfunctional.

Over the past few decades, the incidence of obesity has been increasing worldwide. It has been demonstrated that the intake of a high level of fat is associated with increased cardio-vascular disease risks (24,25), and lipotoxicity is detrimental to numerous cell types, including myocytes, hepatocytes and β cells (26,27). A number of studies have investigated lipotoxicity in cardiomyocytes (28-30). Although a similar phenomenon of decreased autophagy as a result of exposure to a HFD has been demonstrated in other cell types, including proximal tubule cells, embryonic stem cells and neurons (26,31,32), there have been few reports investigating the association between autophagy and obesity. In the present study mice were exposed to a HFD similar to that of obese humans to investigate the role that autophagy serves.

The mechanism through which HFD-induced obesity impairs cardiac function may be multifactorial. The results of the present study demonstrated that the ER served an important role in this process, which is consistent with another study (33). However, the results of the present study indicated that the level of autophagy was decreased in HFD mice, which may be due to the metabolic ER sensor that suppresses the alternative activation of macrophages in obesity (34), as the density of macrophages is associated with autophagy (35). However, the results of the present study were in contrast to

the study by Kong *et al* (36), which instead demonstrated that ERS enhances the level of autophagy. This contradiction may due to the long-term HFD weakening the effect of ERS on macrophages.

In the present study, autophagy was aberrant in HFD-fed mice. An increase in the expression of Atg7 and beclin-1 was observed. However, a HFD decreased the expression of LC3-II/I and increased the expression of P62. Although beclin-1 may stimulate autophagy at an early stage, this does not indicate that HFD-fed mice exhibit an improved autophagic system, as autophagy is followed by fusion with lysosomes and the degradation of the contents. Consistent with the results of the electron microscopy, autophagosomes increased and autolysosomes decreased in the heart tissues of HFD-fed mice, which indicated that the formation of autophagosomes was normal or even increased in HFD-fed mice compared with the NC mice; however, the autophagic flux was suppressed in HFD-fed mice. To confirm the results of the animal experiments, H9C2 cells were treated with PA and Baf A1 *in vitro*. The results demonstrated that PA+Baf increased the LC3-II/I ratio and P62 compared with the control at the protein level. Notably, adding PA or Baf A1 alone did not influence the level of LC3-II/I, however, when administered in combination, the level of LC3-II/I was significantly enhanced. In addition, the level of P62 was significantly increased following treatment with Baf A1, PA or Baf A1+PA. This suggested that PA and Baf A1 may exhibit a synergistic effect resulting in the inhibition of fusion between lysosomes and autolysosomes. In addition, the mCherryGFP-LC3 adenovirus transfection demonstrated that PA was able to induce an accumulation of autophagosomes, but autolysosomes were decreased in H9C2, consistent with the treatment with Baf. This indicated that the administration of PA caused a marked decrease in autolysosome density, and was associated with the fluency of autophagic flux. PA-induced impairment of autophagic flux was increased when Baf A1 was added. These results indicated that the accumulation of autophagosomes induced by the HFD was due to inhibition of autophagosome degradation. Furthermore, it may be a compensatory mechanism under long-term HFD for the increasing expression levels of Atg7, Beclin-1, LC3-I and P62 autophagy-associated proteins. There are an increasing number of studies revealing novel information on autophagy, and the understanding of autophagy in the heart is altering.

Upregulation of autophagy in cardiomyocytes is considered to be an adaptive response to stress, including lipopolysaccharide exposure, ischemia/reperfusion and overload-induced cardiac dysfunction, while suppressing the process accelerates heart failure (37,38). On the contrary, downregulation of autophagy may be a sign of functional aberration due to a number of pathological disorders in cardiovascular disease (39,40). However, the role of autophagy in HFD-induced cardiac injury is not well elucidated. Studies have demonstrated that mice receiving a HFD for >16 weeks may exhibit an altered cardiac autophagic response (41,42), and HFD consumption for 24 weeks leads to the impairment of autophagic flux, primarily due to the disruption of autophagosome degradation (43). Furthermore, a HFD study performed to investigate cardiac function revealed that autophagy was decreased in mice at a time interval of 44 weeks of HFD administration compared with 24 weeks, and that mice who has been administered a HFD for 44 weeks exhibited markedly increased myocardial fibrosis and cardiac hypertrophy (44). Based on these studies and the aim to investigate the role of autophagy in a longer period of time feeding of high fat diet, following the guidelines of Canadian Council on Animal Care (CCAC) on choosing an appropriate endpoint (45,46), a time interval of 42 weeks was chosen in the present study to represent the humane endpoint, and the animals did not present any signs of pain/suffering/discomfort prior to this time interval. The present study indicated that the duration of HFD consumption may be one of the factors that affect the autophagic response in the heart. The decreased autophagic flux may due to the impaired activity of lysosomal proteolysis.

Mitochondria are critical for cardiomyocyte survival and the maintenance of normal cardiac function. There is evidence demonstrating that mitochondrial dysfunction is an important contributor to the function of heart (47). In addition, impaired autophagic flux suggests compromised mitophagy. A previous study has identified that mitophagy appears to be regulated by three distinct signaling pathways, including FUN14 domain-containing protein 1, BCL2/adenovirus E1B 19 kDa protein-interacting protein 3 and the PINK1/parkin signaling pathways. However, under stress conditions, the PINK1/parkin signaling pathway is the main pathway responsible for clearing dysfunctional mitochondria (48). PINK1 is ubiquitously expressed and localized to the mitochondria. It is essential for the cell to maintain PINK1 expression at a certain level. In neurons, genetic ablation of PINK1 leads to mitochondrial dysfunction (49). Furthermore, PINK1 possesses a distinct, non-redundant function in the surveillance and maintenance of cardiac tissue homeostasis (50). In the present study a decrease in PINK1 was observed, indicating mitochondrial dysfunction and mitophagy blockage in HFD mice. Although the present study detected an increase in parkin, it does not affect mitophagy in the absence of PINK1 (51). Mitochondria are highly dynamic, either undergoing fission/fusion to form small individual units or interconnecting with each other for rapid responses to mitochondrial damages. Considering that mitochondrial fusion prevents mitophagy and may therefore protect myocytes against excessive degradation of mito-chondria (52), the level of Mfn2, a mitochondrial membrane protein, which is expressed abundantly in the heart and is a mediator of mitochondrial fusion, was tested. In addition, it is

downstream of PINK1. The results demonstrated a decrease in Mfn2 in the mitochondria of obese mice, which demon-strated that HFD may damage the mitochondrion through the inhibition of mitophagy and mitochondrial fusion. However, the activation of other pathways that can induce mitophagy and other mediators acting on parkin, except PINK1, were not analyzed in the present study.

In addition, the hemodynamic measurements of a total of 7 mice per group were investigated; however, one mouse succumbed to mortality in the normal fat diet group (mortality rate, 14.29%), whereas two mice succumbed to mortality in the HFD group (mortality rate, 28.57%) following the termination of hemodynamic measurements which is consistent with the findings of Mattson (53). Reasons for such mortalities we speculated are mainly because this intravascular process is invisible and it may lead to the rupture of blood vessels or the heart. In addition, Calligaris et al (54) revealed that mice fed with a high-fat diet for a prolonged duration of time presented reduced aortic vasoconstriction and reduced contractile response, which suggested that HFD may affect vascular function and increase the difficulty of PV measurement in HFD mice.

In conclusion, a HFD has been demonstrated to induce dyslipidemia and cardiac dysfunction. These effects may be mediated by the upregulation of ERS, and the downregulation of autophagy and mitophagy in the HFD hearts. However, an investigation into how to reduce the dyslipidemia and dysfunction caused by HFD were not included in the present study. Nevertheless, the results of the present study indicated that autophagy and mitophagy served an important role in HFD-induced cardiomyopathy.

Acknowledgements

Funding

Availability of data and materials

The datasets used and/or analyzed during the current study are available from the corresponding author on reasonable request.

Authors' contributions

YC, Z-PW, YY, NZ and Y-GJ performed the study, analyzed and interpreted the data, and wrote the manuscript. YC, NZ and Q-ZT conceived the hypothesis and participated in the experimental design. YC, Z-PW, YY and C-XW participated in the data interpretation and manuscript drafting. All authors approved final version of the manuscript.

Ethics approval and consent to participate

All the experimental procedures were approved by the Animal Care and Use Committee of Renmin Hospital of Wuhan University, and were in accordance with the Guide for the

Care of Laboratory Animals published by the US National Institutes of Health (publication no. 85-23, revised in 1996).

Consent for publication

Not applicable.

Competing interests

The authors declare that they have no competing interests.

References

1. Hanley AJ, Harris SB, Gittelsohn J, Wolever TM, Saksvig B and Zinman B: Overweight among children and adolescents in a Native Canadian community: Prevalence and associated factors. Am J Clin Nutr 71: 693-700, 2000.
2. Schell LM and Gallo MV: Overweight and obesity among North American Indian infants, children, and youth. Am J Hum Biol 24: 302-13, 2012.
3. von Sarnowski B, Putaala J, Grittner U, Gaertner B, Schminke U, Curtze S, Huber R, Tanislav C, Lichy C, Demarin V, *et al*: Lifestyle risk factors for ischemic stroke and transient ischemic attack in young adults in the stroke in Young Fabry patients study. Stroke 44: 119-125, 2013.
4. Mu Y, Yan WJ, Yin TL, Zhang Y, Li J and Yang J: Diet-induced obesity impairs spermatogenesis: A potential role for autophagy. Sci Rep 7: 43475, 2017.
5. Deng X, Xie Y and Zhang A: Advance of autophagy in chronic kidney diseases. Ren Fail 39: 306-313, 2017.
6. Rezabakhsh A, Cheraghi O, Nourazarian A, Hassanpour M, Kazemi M, Ghaderi S, Faraji E, Rahbarghazi R, Avci ÇB, Bagca BG and Garjani A: Type 2 diabetes inhibited human mesenchymal stem cells angiogenic response by over-activity of the autophagic pathway. J Cell Biochem 118: 1518-1530, 2017.
7. Xu X and Ren J: Unmasking the janus faces of autophagy in obesity-associated insulin resistance and cardiac dysfunction. Clin Exp Pharmacol Physiol 39: 200-208, 2012.
8. Quan W, Jung HS and Lee MS: Role of autophagy in the progression from obesity to diabetes and in the control of energy balance. Arch Pharm Res 36: 223-229, 2013.
9. Wu J, Kong F, Pan Q, Du Y, Ye J, Zheng F, Li H and Zhou J: Autophagy protects against cholesterol-induced apoptosis in pancreatic β-cells. Biochem Biophys Res Commun 482: 678-685, 2017.
10. Starobinets H, Ye J, Broz M, Barry K, Goldsmith J, Marsh T, Rostker F, Krummel M and Debnath J: Antitumor adaptive immunity remains intact following inhibition of autophagy and antimalarial treatment. J Clin Invest 126: 4417-4429, 2016.
11. Contreras AV, Torres N and Tovar AR: PPAR-α as a key nutritional and environmental sensor for metabolic adaptation. Adv Nutr 4: 439-452, 2013.
12. van der Krieken SE, Popeijus HE, Mensink RP and Plat J: Link between ER-stress, PPAR-alpha activation and BET inhibition in relation to apolipoprotein A-I transcription in HepG2 cells. J Cell Biochem 118: 2161-2167, 2017.
13. Marciniak SJ, Yun CY, Oyadomari S, Novoa I, Zhang Y, Jungreis R, Nagata K, Harding HP and Ron D: CHOP induces death by promoting protein synthesis and oxidation in the stressed endoplasmic reticulum. Genes Dev 18: 3066-3077, 2004.
14. Lewy TG, Grabowski JM and Bloom ME: BiP: Master regulator of the unfolded protein response and crucial factor in flavivirus biology. Yale J Biol Med 90: 291-300, 2017.
15. Sha H, He Y, Yang L and Qi L: Stressed out about obesity: IRE1α-XBP1 in metabolic disorders. Trends Endocrinol Metab 22: 374-381, 2011.
16. Wang H, Sun RQ, Camera D, Zeng XY, Jo E, Chan SM, Herbert TP, Molero JC and Ye JM: Endoplasmic reticulum stress up-regulates Nedd4-2 to induce autophagy. FASEB J 30: 2549-2556, 2016.
17. Pankiv S, Clausen TH, Lamark T, Brech A, Bruun JA, Outzen H, Øvervatn A, Bjørkøy G and Johansen T: p62/SQSTM1 binds directly to Atg8/LC3 to facilitate degradation of ubiquitinated protein aggregates by autophagy. J Biol Chem 282: 24131-24145, 2007.
18. Liang XH, Jackson S, Seaman M, Brown K, Kempkes B, Hibshoosh H and Levine B: Induction of autophagy and inhibition of tumorigenesis by beclin 1. Nature 402: 672-676, 1999.
19. Guan H, Yang H, Yang M, Yanagisawa D, Bellier JP, Mori M, Takahata S, Nonaka T, Zhao S and Tooyama I: Mitochondrial ferritin protects SH-SY5Y cells against H2O2-induced oxidative stress and modulates α-synuclein expression. Exp Neurol 291: 51-61, 2017.
20. Braun RJ and Westermann B: With the help of MOM: Mitochondrial contributions to cellular quality control. Trends Cell Biol 27: 441-452, 2017.
21. Bernardini JP, Lazarou M and Dewson G: Parkin and mitophagy in cancer. Oncogene 36: 1315-1327, 2017.
22. Zhao C, Chen Z, Xu X, An X, Duan S, Huang Z, Zhang C, Wu L, Zhang B, Zhang A, *et al*: Pink1/Parkin-mediated mitophagy play a protective role in cisplatin induced renal tubular epithelial cells injury. Exp Cell Res 350: 390-397, 2017.
23. Fang D, Yan S, Yu Q, Chen D and Yan SS: Mfn2 is required for mitochondrial development and synapse formation in human induced pluripotent stem Cells/hiPSC derived cortical neurons. Sci Rep 6: 31462, 2016.
24. Adachi C, Yamanaka-Okumura H, Katayama T, Taketani Y and Takeda E: Single vegetable meal content equivalence as an alternative to fat for satiety: A randomised trial in Japanese women. Asia Pac J Clin Nutr 25: 478-486, 2016.
25. De Lorenzo A, Bernardini S, Gualtieri P, Cabibbo A, Perrone MA, Giambini I and Di Renzo L: Mediterranean meal versus Western meal effects on postprandial ox-LDL, oxidative and inflammatory gene expression in healthy subjects: A randomized controlled trial for nutrigenomic approach in cardiometabolic risk. Acta Diabetol 54: 141-149, 2017.
26. Takabatake Y, Yamamoto T and Isaka Y: Stagnation of autophagy: A novel mechanism of renal lipotoxicity. Autophagy 13: 775-776, 2017.
27. Hao T, Zhang H, Li S and Tian H: Glucagon-like peptide 1 receptor agonist ameliorates the insulin resistance function of islet β cells via the activation of PDX-1/JAK signaling transduction in C57/BL6 mice with high-fat diet-induced diabetes. Int J Mol Med 39: 1029-1036, 2017.
28. Zheng P, Xie Z, Yuan Y, Sui W, Wang C, Gao X, Zhao Y, Zhang F, Gu Y, Hu P, *et al*: Plin5 alleviates myocardial ischaemia/reperfusion injury by reducing oxidative stress through inhibiting the lipolysis of lipid droplets. Sci Rep 7: 42574, 2017.
29. Sakamoto A, Saotome M, Hasan P, Satoh T, Ohtani H, Urushida T, Katoh H, Satoh H and Hayashi H: Eicosapentaenoic acid ameliorates palmitate-induced lipotoxicity via the AMP kinase/dynamin-related protein-1 signaling pathway in differentiated H9c2 myocytes. Exp Cell Res 351: 109-120, 2017.
30. Qin H, Zhang Y, Wang R, Du X, Li L and Du H: Puerarin suppresses Na+-K+-ATPase-mediated systemic inflammation and CD36 expression, and alleviates cardiac lipotoxicity in vitro and in vivo. J Cardiovasc Pharmacol 68: 465-472, 2016.
31. Rhee JS, Saben JL, Mayer AL, Schulte MB, Asghar Z, Stephens C, Chi MM and Moley KH: Diet-induced obesity impairs endometrial stromal cell decidualization: A potential role for impaired autophagy. Hum Reprod 31: 1315-1326, 2016.
32. Komatsu M, Waguri S, Chiba T, Murata S, Iwata J, Tanida I, Ueno T, Koike M, Uchiyama Y, Kominami E and Tanaka K: Loss of autophagy in the central nervous system causes neurodegeneration in mice. Nature 441: 880-884, 2006.
33. Li SJ, Liu CH, Chu HP, Mersmann HJ, Ding ST, Chu CH, Wang CY and Chen CY: The high-fat diet induces myocardial fibrosis in the metabolically healthy obese minipigs-The role of ER stress and oxidative stress. Clin Nutr 36: 760-767, 2017.
34. Shan B, Wang X, Wu Y, Xu C, Xia Z, Dai J, Shao M, Zhao F, He S, Yang L, *et al*: The metabolic ER stress sensor IRE1α suppresses alternative activation of macrophages and impairs energy expenditure in obesity. Nat Immunol 18: 519-529, 2017.
35. Xu X and Ren J: Macrophage migration inhibitory factor (MIF) knockout preserves cardiac homeostasis through alleviating Akt-mediated myocardial autophagy suppression in high-fat diet-induced obesity. Int J Obes (Lond) 39: 387-396, 2015.
36. Kong FJ, Wu JH, Sun SY and Zhou JQ: The endoplasmic reticulum stress/autophagy pathway is involved in cholesterol-induced pancreatic β-cell injury. Sci Rep 7: 44746, 2017.
37. Zhang J, Zhao P, Quan N, Wang L, Chen X, Cates C, Rousselle T and Li J: The endotoxemia cardiac dysfunction is attenuated by AMPK/mTOR signaling pathway regulating autophagy. Biochem Biophys Res Commun 492: 520-527, 2017.

38. Hashemzaei M, Entezari Heravi R, Rezaee R, Roohbakhsh A and Karimi G: Regulation of autophagy by some natural products as a potential therapeutic strategy for cardiovascular disorders. Eur J Pharmacol 802: 44-51, 2017.
39. Hariharan N, Zhai P and Sadoshima J: Oxidative stress stimulates autophagic flux during ischemia/reperfusion. Antioxid Redox Signal 14: 2179-2190, 2011.
40. Zhao D, Wang W, Wang H, Peng H, Liu X, Guo W, Su G and Zhao Z: PKD knockdown inhibits pressure overload-induced cardiac hypertrophy by promoting autophagy via AKT/mTOR pathway. Int J Biol Sci 13: 276-285, 2017.
41. Ceylan-Isik AF, Kandadi MR, Xu X, Hua Y, Chicco AJ, Ren J and Nair S: Apelin administration ameliorates high fat diet induced cardiac hypertrophy and contractile dysfunction. J Mol Cell Cardiol 63: 4-13, 2013.
42. Cui M, Yu H, Wang J, Gao J and Li J: Chronic caloric restriction and exercise improve metabolic conditions of dietary-induced obese mice in autophagy correlated manner without involving AMPK. J Diabetes Res 2013: 852754, 2013.
43. Hsu HC, Chen CY, Lee BC and Chen MF: High-fat diet induces cardiomyocyte apoptosis via the inhibition of autophagy. Eur J Nutr 55: 2245-2254, 2016.
44. Wang Z, Li L, Zhao H, Peng S and Zuo Z: Chronic high fat diet induces cardiac hypertrophy and fibrosis in mice. Metabolism 64: 917-925, 2015.
45. Canadian Council on Animal Care: Guide to the care and use of experimental animals. Ottawa ON, CCAC, Vol. 1, 2nd Edn, pp212, 1993.
46. Hamm TE: Proposed institutional animal care and use committee guidelines for death as an endpoint in rodent studies. Contemporary Topics Lab Animal Sci 34: 69-71, 1995.
47. Aroor AR, Mandavia C, Ren J, Sowers JR and Pulakat L: Mitochondria and oxidative stress in the cardiorenal metabolic syndrome. Cardiorenal Med 2: 87-109, 2012.
48. Rüb C, Wilkening A and Voos W: Mitochondrial quality control by the Pink1/Parkin system. Cell Tissue Res 367: 111-123, 2017.
49. Wood-Kaczmar A, Gandhi S, Yao Z, Abramov AY, Miljan EA, Keen G, Stanyer L, Hargreaves I, Klupsch K, Deas E, et al: PINK1 is necessary for long term survival and mitochondrial function in human dopaminergic neurons. PLoS One 3: e2455, 2008.
50. Billia F, Hauck L, Konecny F, Rao V, Shen J and Mak TW: PTEN-inducible kinase 1 (PINK1)/Park6 is indispensable for normal heart function. Proc Natl Acad Sci USA 108: 9572-9577, 2011.
51. Vives-Bauza C, Zhou C, Huang Y, Cui M, de Vries RL, Kim J, May J, Tocilescu MA, Liu W, Ko HS, et al: PINK1-dependent recruitment of Parkin to mitochondria in mitophagy. Proc Natl Acad Sci USA 107: 378-383, 2010.
52. Gomes LC, Di Benedetto G and Scorrano L: During autophagy mitochondria elongate, are spared from degradation and sustain cell viability. Nat Cell Biol 13: 589-598, 2011.
53. Mattson DL: Long-term measurement of arterial blood pressure in conscious mice. Am J Physiol 274: R564-R570, 1998.
54. Calligaris SD, Lecanda M, Solis F, Ezquer M, Gutiérrez J, Brandan E, Leiva A, Sobrevia L and Conget P: Mice long-term high-fat diet feeding recapitulates human cardiovascular alterations: An animal model to study the early phases of diabetic cardiomyopathy. PLoS One 8: e60931, 2013.